

Received June 29, 2021, accepted July 14, 2021, date of publication July 19, 2021, date of current version July 26, 2021.

Digital Object Identifier 10.1109/ACCESS.2021.3098333

# Development of Ingestible Thermometer With Built-in Coil Antenna Charged by Gastric Acid Battery and Demonstration of Long-Time in Vivo Telemetry

SHINYA YOSHIDA<sup>1</sup>, (Member, IEEE), HIROSHI MIYAGUCHI<sup>2</sup>,  
AND TSUTOMU NAKAMURA<sup>3</sup>, (Member, IEEE)

<sup>1</sup>Graduate School of Engineering, Tohoku University, Sendai 980-8579, Japan

<sup>2</sup>Micro System Integration Center, Tohoku University, Sendai 980-8579, Japan

<sup>3</sup>Promotion Office of Strategic Innovation, Tohoku University, Sendai 980-8579, Japan

Corresponding author: Shinya Yoshida (s-yoshida@tohoku.ac.jp)

This work was supported in part by Japan Science and Technology Agency (JST) Center of Innovation (COI) under Grant JPMJCE1303, and in part by the TERUMO Life Science Foundation.

This work involved human subjects or animals in its research. Approval of all ethical and experimental procedures and protocols was granted by the Institutional Animal Care and Use Committee, Ina Research Inc., under Approval No. 21016.

**ABSTRACT** A safe and affordable ingestible thermometer measuring core body temperature has the potential to become a future healthcare device for versatile applications in daily life. In this study, we developed an ingestible thermometer charged by a gastric acid battery. The device can operate in bowels by using the charged energy in multilayer ceramic capacitors as a storage capacitor. Adopting this strategy for energy storage solves the issues related to a conventional button battery: risk of injury to the digestive tract, bad disposability, and degradation. Additionally, to make it easy to assemble a coil antenna and electrical circuits in the device automatically, we developed a fabrication process based on a vertical stacking process of printed circuit boards with coil patterns. The dimensions of the prototyped device were smaller than those of existing ingestible thermometers. In an experiment involving a dog, we successfully recorded the temperature in the digestive tract for 24 h in cycles of approximately 10 or 20 min, using a rectal thermometer and an existing ingestible thermometer as references. The temperature variations in time among our device, rectal thermometer, and existing ingestible thermometer were almost parallel. The recording ability of the core body temperature using our device has the potential to measure basal body temperature during sleep, the circadian rhythm, and fever type easily and robustly in daily life. Our ingestible thermometer is a step toward the development of sensors that can be swallowed for preventive medicine and health promotion.

**INDEX TERMS** Biomedical electronics, biomedical telemetry, components, packaging, manufacturing technology, sensor systems and applications, system integration, temperature measurement, temperature sensors.

## I. INTRODUCTION

Vital sensing or monitoring in daily life has prospects in promoting health and detecting diseases at an early stage. The general vision is referred to as “digital health,” “mobile health,” “Internet of Medical Things,” etc., and it is gradually becoming established among many people because of advances in wearable sensor technologies [1]–[5]. In the

The associate editor coordinating the review of this manuscript and approving it for publication was Chunsheng Zhu<sup>1</sup>.

future, minimally invasive and safer technologies should be developed as next-generation healthcare technology [6], [7].

For example, ingestible sensors, which can be swallowed by a user to monitor vital data in the body, will become a promising technology in the near future [8]–[10]. Thus far, various ingestible sensors have been developed to measure core body temperature [11]–[13], gas [14], microbiome [15], pH [16], pressure [17] and capsule-type imagers [18]. Among them, it is predicted that ingestible thermometers will produce the largest market with a steady growth rate [19]. One reason

for this prediction is that core body temperature and its temporal patterns, especially during sleep, are fundamental vital signs, and thus can be used for various purposes. Hence, their monitoring and logging can potentially help to detect various diseases earlier or more accurately, such as menstrual disorders [20], polycystic-ovary syndrome [21], depression [22], infection [23], and a specific sleep disorder [24], [25]. In addition, the core body-temperature rhythm is a strong indicator of the circadian rhythm (inner-body clock). In particular, it is important to observe the timing of the lowest body temperature during sleep because it is an indicator of the phase of the rhythm. An abnormal phase shift from the sleep-wake rhythm and/or social clock increases the risk of disordered sleep, cancer, obesity, depression, diabetes, infertility, etc. [26]–[29]. Mental and athletic performance also strongly depends on the rhythm [30], [31]. Thus, aggressive monitoring and calibration contribute not only to disease therapy and diagnosis, but also to empowerment. An attractive advantage of the ingestible thermometer is that it can obtain reliable data more robustly to the environmental or contact conditions compared with other non-contact or contact-type sensors. It has been proven that it is possible to accurately measure body temperature, which is strongly correlated with rectal temperature [23], [32].

Ingestible thermometers are already commercially available. However, these sensors have a critical problem: they use button batteries as energy sources. Hence, these existing devices have a risk of causing severe injuries, such as damage to the gastrointestinal tract due to the discharge current or toxic electrolyte if the button battery is exposed inside the body. Issues of disposability and self-discharge also arise with the fabrication of devices using primary batteries. Wireless power from the outside of the body to an ingested device has been proposed [11]. However, difficulty may arise in efficiently supplying power to a device whose position is unknown in the body. Consequently, large exposure amounts of electromagnetic radiation to the body may be required to supply sufficient power, which poses further health risks. In addition, these devices are too expensive for consumer use. These problems may limit the use of the device in specialized applications, such as in athletics or the military.

Thus, in previous studies, we developed a core-body thermometer based on gastric acid power generation even after the device has passed through the stomach, as shown in Fig. 1 [33]–[35]. The gastric acid power generation charges electrical energy into a storage capacitor, which is safer than a button battery, in the device. This concept reduces the environmental burden of disposing of the device after use. Since the device is spontaneously charged when taken, there is no need to worry about deterioration like button batteries. Thus, the device has quality robustness to product design, and the restrictions of logistics and storage conditions are minimized.

The idea of using gastric acid power generation has been considered for a long time. Medication management devices

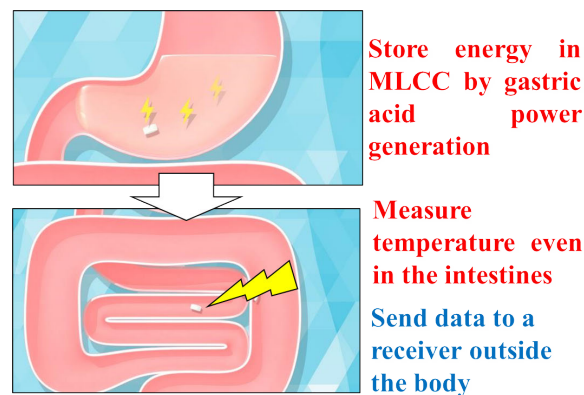


**FIGURE 1.** Schematic illustration of the ingestible thermometer based on gastric acid battery.

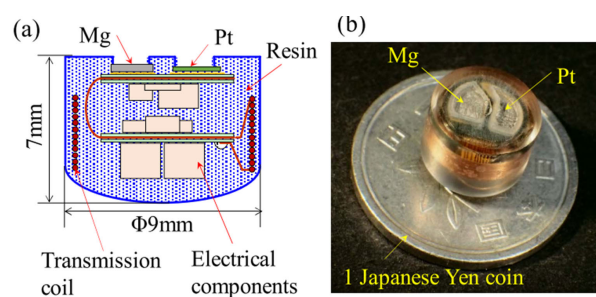


**FIGURE 2.** Previous device utilizing a folded rigid flexible PCB and a separate coil. (a) Cross-sectional schematic. (b) Picture of the device [35].

are a recent example [36], [37]. An ingestible thermometer that is meant to remain within the stomach for a long time has been reported [39]. However, these devices are assumed to be operated only in the stomach because the power generation virtually stops in the bowels. The average residence time in the stomach is approximately 1 h. Thus, the designs of these systems do not meet our intended application, that is, observation of temporal patterns of core body temperature for ten or more hours. In a previous study, we successfully prototyped a tablet-shaped device and demonstrated *in vivo* telemetry by letting a dog swallow the device [35]. However, the device was fabricated by folding a rigid-flexible circuit board, as shown in Fig. 2. The coil antenna was mounted manually. These complicated assembly processes make automatic fabrication difficult and prevent the reduction of the fabrication cost. Our goal is to supply a device for various applications in consumer use by cost-effective mass production. Moreover, long-time operation, such as more than 10 h, has not yet been demonstrated. Thus, our concept has not yet been completely proven.

Therefore, in this study, we designed a suitable structure for an ingestible thermometer with superior mass-production, and then prototyped the device. We then demonstrated *in vivo* telemetry for a long time.

## II. SYSTEM DESIGN

Fig. 3 depicts a system diagram of the ingestible thermometer proposed in this study. When the device is ingested, power

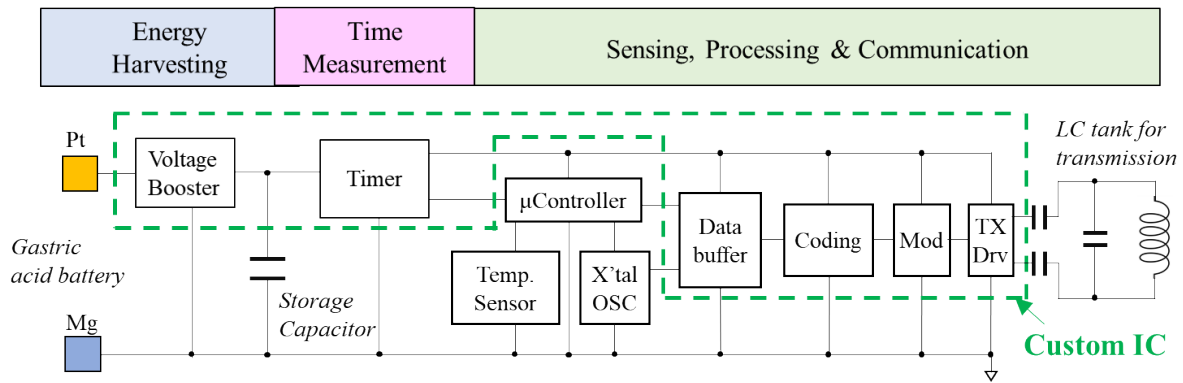


**FIGURE 3.** System outline of the ingestible thermometer based on gastric acid power generation. The parts inside the dashed green line were implemented in a custom IC.

generation starts by bringing the electrodes (e.g., Mg and Pt electrodes) into contact with a gastric acid fluid, and then drives a self-excited-oscillating circuit for voltage boosting. Subsequently, a clock pulse drives a voltage boost circuit, and the electric energy is charged in a multilayer ceramic capacitor (MLCC) at the boosted voltage. An MLCC was chosen as a storage capacitor because it is inexpensive, easy to procure, safe for the body because of the absence of a toxic electrolytic solution, and can be charged quickly. The charged energy becomes an energy source for this system after it passes through the stomach. The timer circuit manages the operation timing of the subsequent elements, such as temperature sensing and telecommunication functions. When a preset timing arrives, the charged energy is supplied to them. A general-purpose microcontroller obtains temperature data from a temperature sensor through an inter-integrated circuit interface. The microcontroller then creates a data packet and sends it to a data buffer. The data are bit-rate converted, encoded, modulated, and eventually sent to an external receiver via magnetic-field coupling communication. This communication method does not require adhesives or direct contact between the receiver and skin to receive data from the ingested device. In this study, an 11.3-MHz carrier frequency generated by a crystal oscillator was used because such a relatively low radio-frequency carrier should have a well-balanced performance between biological permeability and efficiency as a limited-size transmission antenna in the ingestible device. This contributes to ensuring safety in the human body and reducing energy consumption in telecommunications. The 13.56 MHz carrier wave is often used for short-range wireless communications. However, the carrier wave of 13.56 MHz had a relatively high background noise level in the ambient environment of the laboratory. Therefore, in this study, the 11.3 MHz carrier wave was selected to achieve reliable communication.

To minimize the driving energy loss, an LC parallel resonant circuit, which is driven by differential outputs, is used to generate a modulated magnetic field. Manchester encoding and binary phase-shift keying (BPSK) were adopted as the

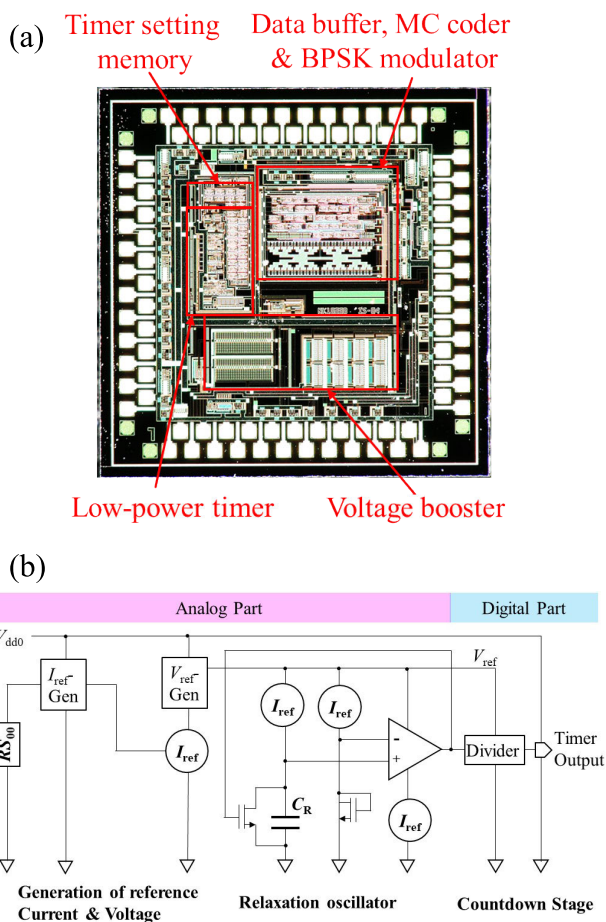
encoding and modulating methods, respectively. The content of the data packet is described in our previous study [34].

Some functional elements were implemented in a custom integrated circuit (IC) (inside the dashed green line in Fig. 3). This contributes not only to miniaturization of the device, but also to reducing the energy consumption for the encoding and modulating processes. Fig. 4 (a) is the photograph of the chip of the custom IC. The die was a square with a side length of 1.8 mm. A conventional 0.5- $\mu\text{m}$  CMOS process was employed for cost reduction and to ensure a wide range of operating voltages. The circuit design of the voltage booster is described in [38]. The chargeable energy in an MLCC is several orders of magnitude lower than that of general button batteries. Thus, energy saving is required for not only the active mode (temperature sensing and telecommunication, etc.), but also for the non-active mode. Therefore, an ultralow-power timer circuit was implemented in this custom IC.

Figure 4(b) shows the block diagram of the timer circuit. This is composed of analog and digital parts. The former oscillates a fundamental frequency as a clock. The latter counts the clock for determining a timer period. A constant current source circuit ( $I_{\text{ref-Gen}}$ ) is driven by the voltage ( $V_{\text{dd0}}$ ) supplied from the storage capacitor, and then generates a reference current ( $I_{\text{ref}}$ ) defined by the external resistance ( $RS_{00}$ ). Then, a constant voltage source circuit ( $V_{\text{ref-Gen}}$ ) generates a reference voltage ( $V_{\text{ref}}$ ) from the reference current. As a result, the following circuit elements operate at  $V_{\text{ref}}$  as a power-supply voltage. The oscillation circuit adapts a configuration of a relaxation oscillation circuit. The output of the oscillator is connected to the digital part through the comparator and divider, and eventually becomes the timer output. In this study, the reference current itself was reduced by setting a large external resistance ( $RS_{00}$ ) such as more than 10 M $\Omega$ . In addition, the number of circuit elements consuming the current was also reduced as much as possible. As a result, the power consumption of the timer circuit was as small as  $\sim 7.5$  nA at 4 V. The period of the timer in the custom IC can be set by the timer set memory, which is written by the microcontroller.

**TABLE 1.** Physical and technical characteristics of the ingestible thermometers [12].

Product name (Developer) or Research group	CorTemp (HQ. Inc.)	e-Celsius (BodyCap)	myTemp (myTemp BV)	VitalSense (Royal Philips)	P. Nadeau et al. [39]	This work
Dimensions	10.9 mm (Φ)	8.9 mm (Φ)	8.0 mm (Φ)	8.7 mm (Φ)	>10 mm (Φ)	8.3 mm (W) ×
	22.4 mm (L)	17.7 mm (L)	20.0 mm (L)	23.0 mm (L)	>30 mm (L)	6.0 mm (H) ×
Weight	2.8 g	1.7 g	1.3 g	1.5 g	-	14.3 mm (L) ×
Power source	Silver oxide battery	Silver oxide battery	Extracorporeal wireless power transfer	Silver oxide battery	Gastric acid battery	Gastric acid battery

**FIGURE 4.** (a) Photograph of the chip of the custom IC (0.5  $\mu\text{m}$ /5 V CMOS process). The chip size is 1.9mm  $\times$  1.9mm. (b) Block diagram of the low power timer.

### III. FABRICATION OF DEVICE

Fig. 5 illustrates the fabrication flow of the device. A coil pattern was formed on the outer periphery of the components. First, on PCB-B, a Pt thin film was electrically plated on the Au pads as a positive electrode of the gastric acid battery in advance. All electronic components, except the custom IC, were then mounted on rigid PCBs (PCB-A and PCB-B), and the bare chip of the custom IC was mounted with wire

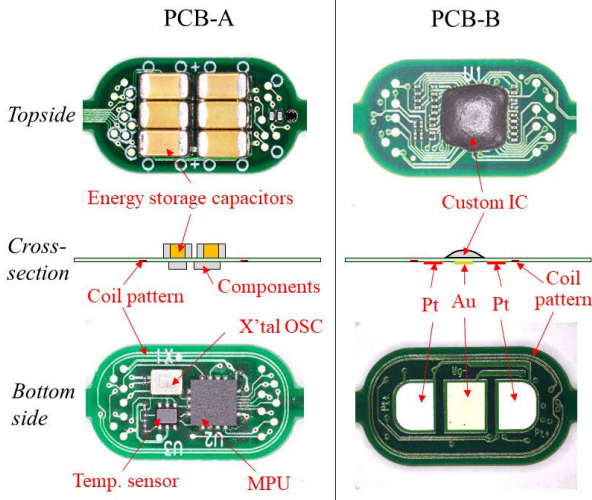
bonding, as shown in Fig. 5(1). In this study, PIC16LF1503 (Microchip Technology Inc.), TMP112 (Texas Instruments Inc.), and KC2016K (Kyocera Corp.) were used as the microcontroller, temperature sensor, and crystal oscillator, respectively. The accuracy and resolution of the temperature sensor were 0.5  $^{\circ}\text{C}$  and 0.0625  $^{\circ}\text{C}$ , respectively. Six pieces of MLCC with nominal capacitance of 220  $\mu\text{F}$  were mounted as the storage capacitors. The PCBs were stacked and electrically connected via an intermediate PCB (labeled “PCB-Mid”) by a soldering reflow process, as shown in Fig. 5(2). PCB-Mid not only had an embedded multilayer coil pattern, but also prevented the interference of components on PCB-A and PCB-B. The device was then cut out, as shown in Fig 5(3). Then, a 250- $\mu\text{m}$ -thick Mg plate was bonded via an Ag paste. Finally, the PCBs were packaged with epoxy resin. Only the Mg–Pt electrodes are exposed for contact with gastric acid.

Various approaches have been reported for the implementation and layout of antennas on ingestible devices [40]–[44]. Helical or spiral antennas by utilizing PCB technologies were also reported [45], [46]. As seen in Fig. 5, advantages of the assemble process in this study is scalable and compatible with a standard solder-reflow process. Many devices with embedded coils can be manufactured at once with large PCBs. This process can be easily conducted by the company that mounts electronic components. Moreover, this simple process based on just stacking PCBs from one direction is suitable for automation by a machine. These will contribute to the cost reduction in the device production. The cost of the electronic components used is also low, which should lead to the supply of affordable devices.

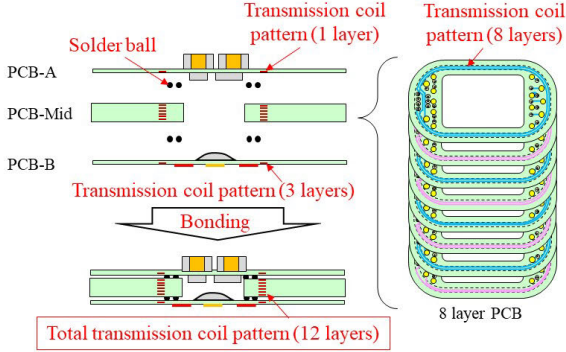
Fig. 6 (a) depicts images of the prototype device. The dimensions were 14.3 (length)  $\times$  8.3 (width)  $\times$  6.0 (height) mm. This device was smaller than existing commercial ingestible thermometers. Table 1 shows the comparison of existing ingestible thermometers, our prototyped device in this study, and the device powered by a gastric acid battery reported by other research group [39]. The work of [39] was much larger than our device although a gastric acid battery was employed. Such a large size was caused by use of only the general-purpose ICs and electrical components. In addition, they were mounted on a relatively-large PCB. Thus, the size reduction was limited. By contrast, our device was assembled



(1) Prepare PCBs mounted with electrical components



(2) Stack PCBs and electrically connect with solder ball



(3) 1. Cut out devices, 2. mount Mg plate, and 3. package with a resin

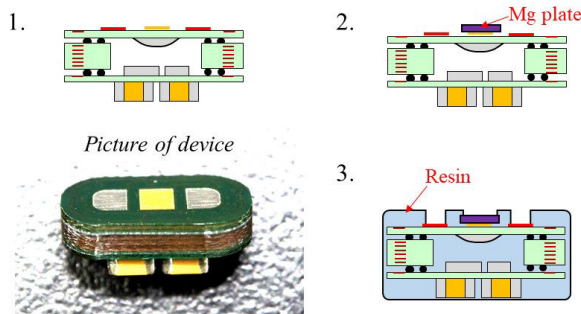


FIGURE 5. Fabrication process of the ingestible thermometer utilizing stacking of PCBs with coil patterns.

by the stacking process, and utilized the specially-designed custom IC with essential functions such as energy harvesting, coding, timer circuits etc. for realizing ingestible devices. Thus, a synergy effect of elimination of a button battery, use of custom IC and adapt of the sophisticated assemble process considerably contributed to the miniaturization.

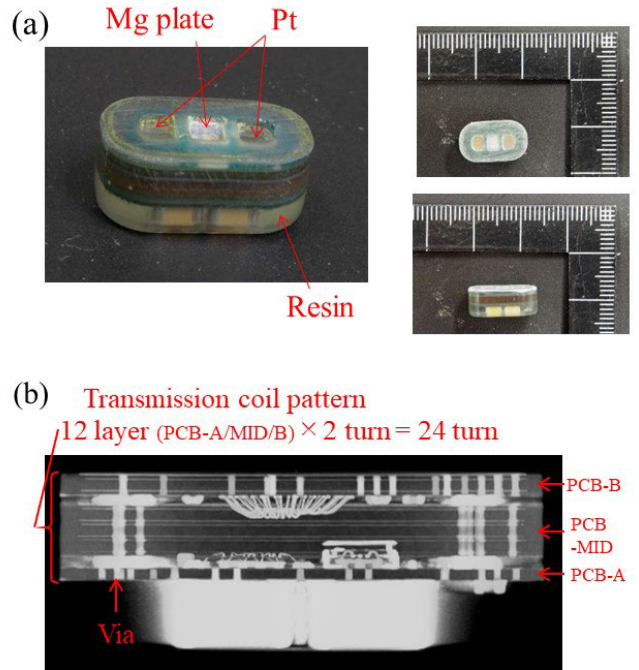


FIGURE 6. (a) Picture of the prototyped device. (b) Cross-sectional view observed by X-ray computed tomography.

Unfortunately, the device size in this study became larger than the tablet-shaped device ( $\varphi 9 \text{ mm} \times 7 \text{ mm}$ ) in our previous study [35] because the capacitance of the storage capacitor was increased for realizing the long-time operation more than 10 hours. Even so, the device size still smaller than other ingestible thermometers. The small size contributes to reducing the risk of leaving the device in the body and of blockage of the digestive tract [8].

The X-ray computed tomography image (Fig. 6(b)) depicts the coil antennas on each layer, which are connected vertically with the vias in the device. The number of turns was 24, and the inductance and resistance were approximately  $6 \mu\text{H}$  and  $14 \Omega$ , respectively.

IV. IN VITRO OPERATION TEST

An operation test of the prototype devices was performed *in vitro* as a preliminary experiment. In this experiment, metal probes were placed on the gastric-acid-battery electrodes of Mg and Pt. Then, 1.2 V was applied for 30 min assuming gastric-acid power generation occurs in the stomach. This applied voltage was increased to approximately 4.2 V by the voltage booster circuit; thus, the MLCC was charged at this voltage. We then stopped the voltage application and observed the performance of the device by using the charged energy, assuming the device moved to the bowels. The data signals transmitted from the device were received by a commercially available magnetic loop antenna (LA400, AOR Ltd). The distance between the device and antenna was estimated to be approximately 20 cm. This experiment was performed under ambient conditions using a general air conditioner. We prepared two samples with a timer circuit

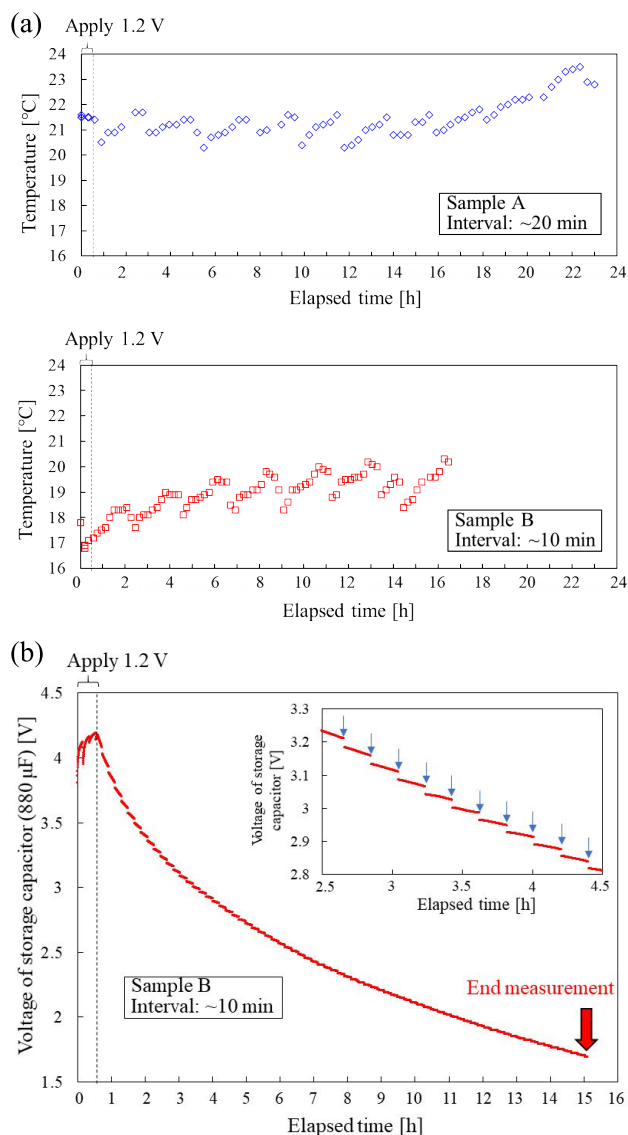


**FIGURE 7.** (a) Operation test results of the devices *in vitro*. The measurement cycles of sample A and sample B are 20 min and 10 min, respectively. (b) the variation of the voltage in time for Sample B before the packaging with the resin. The arrows in the magnified graph indicate the time of the active mode.

interval of approximately 20 min (sample A) and 10 min (sample B). The measurement frequency of the latter device was doubled. In other words, the accumulated energy consumption for the active mode was twice that of the former.

Fig. 7 (a) illustrates the variation of the measured temperature in time in the operation test. The temperature change of the experimental room according to the air-conditioner was monitored. Sample A operated for approximately 23 hours while over 16 hours was achieved in sample B as a measurement time. Note that the operation experiments for each sample were conducted on different days. Therefore, the values of the measured room temperatures are different largely.

Fig. 7 (b) shows the variation of the voltage of the storage capacitor in time for the sample B before it was packaged

with the resin. The voltage was measured in 10 second cycle with a voltmeter by directly contacting the storage capacitor. As well as the experiment of Fig. 7 (a), 1.2 V was applied for 30 min to the electrode pads for the gastric acid battery. As mentioned above, the storage capacitor was charged at approximately 4.2 V. Then, the voltage started to drop after the voltage application ended. In the range of the high voltage, the rate of the voltage drop was relatively high because the power consumption of the system was high when the supply voltage was high. After 15 hours, the voltage of the storage capacitor reached to 1.7 V. Considering that the system can be operated around 1.6~1.8 V, the operation test result shown in Fig. 7 (a) looked reasonable.

As seen in the magnified graph of Fig. 7 (b), the voltage discontinuously dropped at the timing of the “active mode” for one measurement and transmission. Other region corresponding to the “non-active mode” operated with the timer circuit. The energy consumptions for “active mode” in this specimen were estimated to be ~70 μJ around 3 V per single measurement if the nominal capacitance of the storage capacitor (1320 (= 6 × 220) μF) was adapted for the estimation. On the other hand, “non-active mode” was ~60 μJ per ~10 min (i.e. 90~100 nW). In practical, the capacitance of MLCC becomes smaller than the nominal due to DC (direct current) bias characteristics. Thus, the actual energy consumptions were probably smaller. But, these results can be used as a guide for designing a feasible measurement cycle/measurement time relationship based on the capacity of the on-board MLCC.

The existing ingestible thermometers can monitor the temperature in a dozen-second period for a few days. In contrast, the current design of our device measured in periods of the order of minutes for ten or more hours because the available energy of the device using an MLCC is several orders of magnitude smaller than that of a typical button battery. Because the energy charged in the MLCC is limited, there is a trade-off between the maximum measurable time and the number of measurements. However, various applications, such as measurement of basal temperature during sleep, circadian rhythm, and bed-side monitoring of infection patients, probably do not require frequent monitoring. Thus, our device and existing devices are expected to be used differently. In addition, we can expect that advancements in the energy density of MLCCs will further increase the maximum measurable time or measurement frequency in the future.

## V. DEMONSTRATION OF IN VIVO LONG-TIME TELEMTRY

Finally, an *in vivo* telemetry experiment was performed by ingesting the device in a male beagle dog. We first prepared a dog house surrounded by receiver antennas for this experiment, as shown in Fig. 8. A total of six loop antennas were attached; two antennas were each placed on the bottom and the near/far sides. The antenna was connected to a receiver system shown in Fig. 8 (c). The RF raw signal received by the antenna was sent to the analog frontend, demodulating,

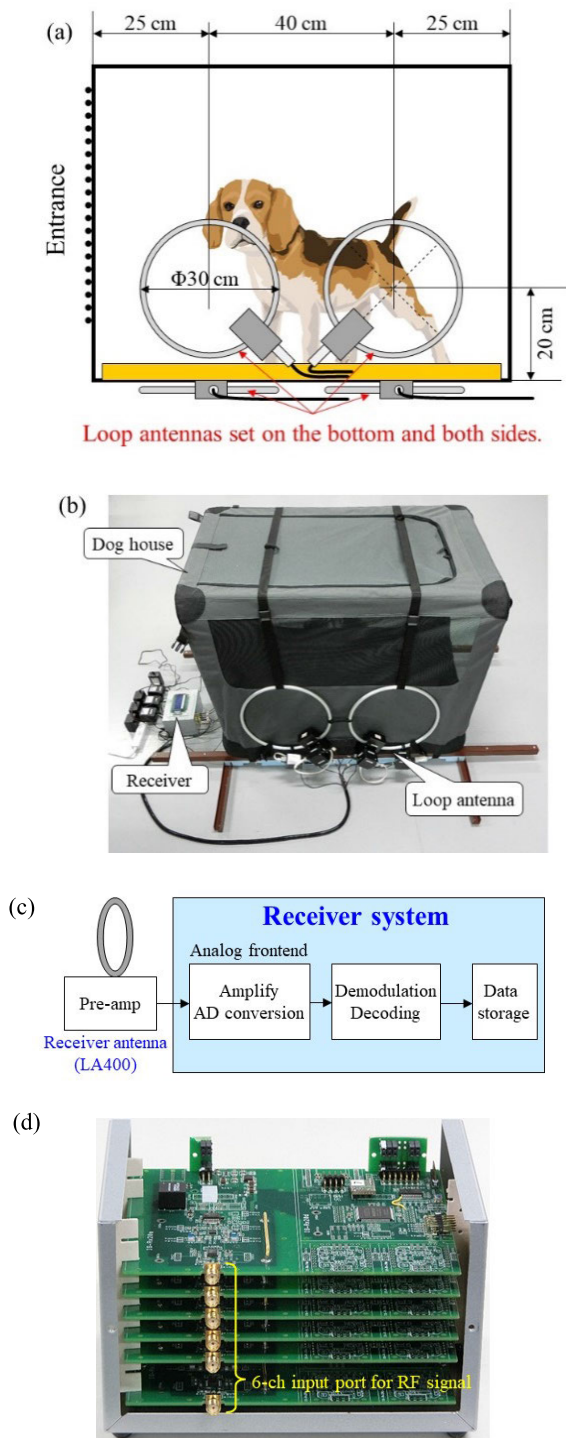


**FIGURE 8.** (a) Schematic illustration of the layout of the receiver antennas for the *in vivo* telemetry with a dog. (b) Picture of the actual setup. (c) Block diagram of the receiver system. (d) Picture of the multi-receiver system with 6-ch input ports for RF signal.

decoding circuits. The data was stored in the memory of the system, and eventually was read out by connecting a personal computer after the experiment was completed. In this experiment, the six receiver systems were prepared and stacked, as seen in Fig. 8 (d) for the parallel reception by the six antennas.

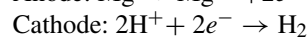
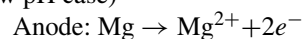
The devices (samples A and B) were then swallowed by the dog. In addition, CorTemp™ (supplied by the HQ. Inc) was used as a reference. Afterward, the dog was put to sleep using a sedating agent (secobarbital sodium), and the dog was put in the dog house. The rectal temperature was also monitored by inserting a thermal probe (CTM-303, Terumo Corporation) during the sleeping state. After approximately 30 min, the rectal thermal probe was removed, and the dog was removed from the dog house and placed on a medical table. The inside of the stomach was observed using an endoscope. Afterward, the dog was put back in the dog house, and the rectal probe was set until the dog became awake during the telemetry. The rectal probe was then removed before the dog became completely awake, and the core-body temperature was monitored using only the ingestible devices for 24 h. The devices stayed in the body and were not excreted during this experiment of 24 hours.

All experimental procedures conformed to “the Act on Welfare and Management of Animals” and “Regulations for Animal Experiments at Ina Research Inc.,” and they were reviewed by the Institutional Animal Care and Use Committee of Ina Research Inc. (Protocol number: 21016, Approval date: January 20, 2021)

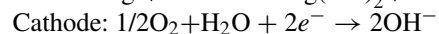
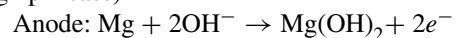
Fig. 9 illustrates the temperature recorded in the measurement experiment. As seen in Fig. 9 (a), the long-time measurement for 24 h was demonstrated successfully. After the sedation, the temperature dropped consistently until 12:00. That looks reasonable because sedation and/or anesthesia normally lower the body temperature. Then, the body temperature gradually increased as the dog became awake, and eventually varied between 38.0 and 39.5 °C.

The operation time of “Sample B” was longer than that of the *in vitro* test results. The device probably stayed and charged in the stomach for a longer time than expected. For at least 30 min after ingestion, all devices were observed in the stomach, as shown in Fig. 9(c). In addition, a power generation from a galvanic effect of the Mg-Pt electrode possibly occurred even in the intestine. The assumed discharge reactions in this battery system are as follows.

(Low pH case)



(High pH case)



An intestinal juice is normally neutral or slightly alkaline, and also an electrolytic solution containing sodium chloride. Thus, a small power was probably generated by consuming proton or oxygen in the juice, and might led to additional slight charge of the storage capacitor.

The temperature variations of our devices, CorTemp™, and the rectal thermometer were almost parallel. The temperature of CorTemp™ always appears to be 0.2 °C–0.3 °C higher than that of our devices. This might be due to the differences in the sensing accuracy among the devices. Alternatively, CorTemp™ might have been slightly heated up



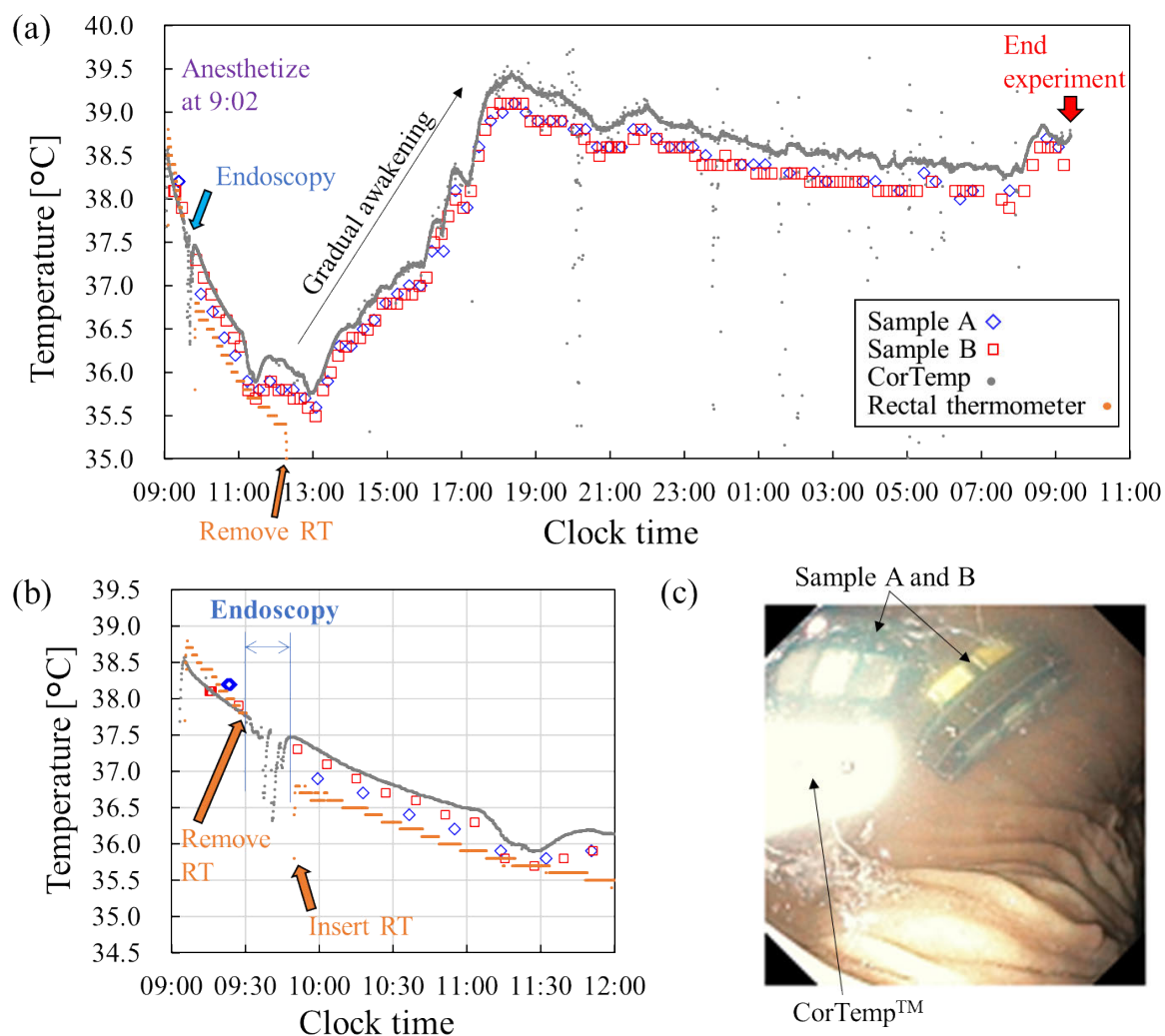


**FIGURE 9.** Demonstration of the *in vivo* telemetry experiment. (a) Raw temperature data recorded for 24 hours. RT means rectal thermometer. (b) Detailed plot of the recorded temperature data under sedation. (c) Endoscopic image of the devices in the stomach.

because of its high-frequency measurement of a few tens of seconds. As seen in Fig. 9 (b), the variation in the rectal temperature shifted before and after the endoscopic observation. The rectal thermometer was then removed for observation. This might indicate that even the rectal temperature was influenced by the contact condition between the inserted probe and the rectal wall or feces. In this experiment, the rectal temperature almost matched the data measured with our devices before the endoscopic observation, and it was 0.2 °C–0.3 °C lower after the observation. This suggests that the ingestible thermometer has the potential to provide a more robust sensing method for the core body temperature. Note that strengths of the electric and magnetic field generated by our ingestible thermometer are roughly estimated to be an order of magnitude lower than the reference level of International Commission on Non-ionizing Radiation Protection. Thus, the electromagnetic waves are not expected to have any effect on the human body.

Therefore, we successfully developed a fabrication process that makes it easy to integrate a coil antenna into an ingestible thermometer. We demonstrated that this thermometer based on gastric acid power generation can measure the core body temperature of a living animal for a long time.

## VI. CONCLUSION

In this study, we prototyped an ingestible thermometer with a built-in coil antenna, whose operation energy is charged by a gastric acid battery. The custom IC implemented with essential functions, such as ultralow-power timer, coding, modulation, and transmission driver circuits, was prepared to realize the conceptual device. We also developed an implementation process for a coil antenna in the device by vertically stacking PCBs with loop patterns. Consequently, the integration and assembly process of all components were considerably simplified compared with the previous method of using rigid-flexible circuit boards [34], [35]. The dimen-



sions of the fabricated device were 14.3 mm (length)  $\times$  8.3 mm (width)  $\times$  6.0 mm (height). This size is smaller than that of other existing ingestible thermometers with general button batteries. Finally, we successfully demonstrated *in vivo* telemetry for 24 h in cycles of approximately 10 or 20 min. The temperature variations in time between our devices and reference sensors were almost parallel. This performance has prospects for easily and robustly measuring basal body temperature during sleep, the circadian rhythm, and fever type. In addition, the resolution and accuracy of the device will be further improved by adopting a higher-accuracy temperature IC in the system. Our device has the potential to become a safe and inexpensive ingestible thermometer that would be more widely used than existing products. We believe that our ingestible thermometer is the first step toward creating an ingestible sensor available in daily life for preventive medicine and health promotion.

## REFERENCES

- [1] J. Tu, R. M. Torrente-Rodríguez, M. Wang, and W. Gao, "The era of digital health: A review of portable and wearable affinity biosensors," *Adv. Funct. Mater.*, vol. 30, no. 29, pp. 1–30, 2020.
- [2] H. Zhang, C. Song, A. S. Rathore, M.-C. Huang, Y. Zhang, and W. Xu, "MHealth technologies towards Parkinson's disease detection and monitoring in daily life: A comprehensive review," *IEEE Rev. Biomed. Eng.*, vol. 14, pp. 71–81, 2021.
- [3] F. Yang, Q. Wu, X. Hu, J. Ye, Y. Yang, H. Rao, R. Ma, and B. Hu, "Internet of Things enabled data fusion method for sleep healthcare applications," *IEEE Internet Things J.*, early access, Mar. 22, 2021, doi: 10.1109/IJOT.2021.3067905.
- [4] N. Van Helleputte, A. J. G. Even, F. Leonardi, S. Stanzione, M. Song, C. Garripoli, W. Sijbers, Y.-H. Liu, and C. Van Hoof, "Miniaturized electronic circuit design challenges for ingestible devices," *J. Microelectromech. Syst.*, vol. 29, no. 5, pp. 645–652, Oct. 2020.
- [5] P. P. Ray, "Intelligent ingestibles: Future of internet of body," *IEEE Internet Comput.*, vol. 24, no. 5, pp. 19–27, Sep. 2020.
- [6] S. Carrara, "Body dust: Well beyond wearable and implantable sensors," *IEEE Sensors J.*, vol. 21, no. 11, pp. 12398–12406, Jun. 2021.
- [7] H. Dinis and P. M. Mendes, "A comprehensive review of powering methods used in state-of-the-art miniaturized implantable electronic devices," *Biosens. Bioelectron.*, vol. 172, Oct. 2020, 2021, Art. no. 112781.
- [8] C. Steiger, A. Abramson, P. Nadeau, A. P. Chandrakasan, R. Langer, and G. Traverso, "Ingestible electronics for diagnostics and therapy," *Nature Rev. Mater.*, vol. 4, no. 2, pp. 83–98, Feb. 2019.
- [9] L. A. Beardslee, G. E. Banis, S. Chu, S. Liu, A. A. Chapin, J. M. Stine, P. J. Pasricha, and R. Ghodssi, "Ingestible sensors and sensing systems for minimally invasive diagnosis and monitoring: The next frontier in minimally invasive screening," *ACS Sensors*, vol. 5, no. 4, pp. 891–910, Apr. 2020.
- [10] A. S. Sharova, F. Melloni, G. Lanzani, C. J. Bettinger, and M. Caironi, "Edible electronics: The vision and the challenge," *Adv. Mater. Technol.*, vol. 6, no. 2, Feb. 2021, Art. no. 2000757.
- [11] C. C. W. G. Bongers, M. T. E. Hopman, and T. M. H. Eijsvogels, "Validity and reliability of the myTemp ingestible temperature capsule," *J. Sci. Med. Sport*, vol. 21, no. 3, pp. 322–326, Mar. 2018.
- [12] C. C. W. G. Bongers, H. A. M. Daanen, C. P. Bogerd, M. T. E. Hopman, and T. M. H. Eijsvogels, "Validity, reliability, and inertia of four different temperature capsule systems," *Med. Sci. Sports Exerc.*, vol. 50, no. 1, pp. 169–175, 2018.
- [13] C. O'Brien, R. W. Hoyt, M. J. Buller, J. W. Castellani, and A. J. Young, "Telemetry pill measurement of core temperature in humans during active heating and cooling," *Med. & Amp Sci. Sports & amp Exerc.*, vol. 30, no. 3, pp. 468–472, Mar. 1998.
- [14] K. Kalantar-Zadeh, K. J. Berean, N. Ha, A. F. Chrimes, K. Xu, D. Grando, J. Z. Ou, N. Pillai, J. L. Campbell, R. Brkljača, K. M. Taylor, R. E. Burgell, C. K. Yao, S. A. Ward, C. S. McSweeney, J. G. Muir, and P. R. Gibson, "A human pilot trial of ingestible electronic capsules capable of sensing different gases in the gut," *Nature Electron.*, vol. 1, no. 1, pp. 79–87, Jan. 2018.
- [15] C. Zhu, Y. Wen, T. Liu, H. Yang, and K. Sengupta, "A packaged ingestible bio-pill with 15-pixel multiplexed fluorescence nucleic-acid sensor and bi-directional wireless interface for *in-vivo* bio-molecular sensing," in *Proc. IEEE Symp. VLSI Circuits*, vol. 10, no. 3, Jun. 2020, pp. 1–2.
- [16] Heidelberg Medical. *Gastric pH Diagnostic System and pH Capsule*. Accessed: May 10, 2021. [Online]. Available: <https://www.phcapsule.com/>
- [17] C. H. Liao, C.-T. Cheng, C.-C. Chen, U.-M. Jow, C.-H. Chen, Y.-L. Lai, Y.-C. Chen, and D.-R. Ho, "An ingestible electronics for continuous and real-time intraabdominal pressure monitoring," *J. Pers. Med.*, vol. 11, no. 1, pp. 1–10, 2021.
- [18] T. Nakamura and A. Terano, "Capsule endoscopy: Past, present, and future," *J. Gastroenterol.*, vol. 43, no. 2, pp. 93–99, Feb. 2008.
- [19] *Ingestible Sensors Market Size, Share & Trends Analysis Report By Vertical (Sports, Medical), By Component (Sensors, Software), By Sensor Type (Temperature, Pressure, Image Sensors), and Segment Forecasts, 2018–2024*, Grand View Res., San Francisco, CA, USA, Jul. 2018.
- [20] A. Palmer, "Basal body temperature determinations in the management of menstrual disorders," *Clin. Obstetrics Gynecol.*, vol. 2, no. 1, pp. 153–179, 1959.
- [21] W. W. Webster and B. Smarr, "Using circadian rhythm patterns of continuous core body temperature to improve fertility and pregnancy planning," *J. Circadian Rhythms*, vol. 18, no. 1, pp. 1–8, Sep. 2020.
- [22] B. P. Hasler, D. J. Buysse, D. J. Kupfer, and A. Germain, "Phase relationships between core body temperature, melatonin, and sleep are associated with depression severity: Further evidence for circadian misalignment in non-seasonal depression," *Psychiatry Res.*, vol. 178, no. 1, pp. 205–207, Jun. 2010.
- [23] F. Huang, C. Magnin, and P. Broquii, "Ingestible sensors correlate closely with peripheral temperature measurements in febrile patients," *J. Infection*, vol. 80, no. 2, pp. 161–166, Feb. 2020.
- [24] M. Morris, L. Lack, and D. Dawson, "Sleep-onset insomniacs have delayed temperature rhythms," *Sleep*, vol. 13, no. 1, pp. 1–14, Jan. 1990.
- [25] L. C. Lack, M. Gradisar, E. J. W. Van Someren, H. R. Wright, and K. Lushington, "The relationship between insomnia and body temperatures," *Sleep Med. Rev.*, vol. 12, no. 4, pp. 307–317, Aug. 2008.
- [26] S. Crnko, B. C. D. Pré, J. P. G. Sluiter, and L. W. Van Laake, "Circadian rhythms and the molecular clock in cardiovascular biology and disease," *Nature Rev. Cardiol.*, vol. 16, no. 7, pp. 437–447, Jul. 2019.
- [27] Y. Leng, E. S. Musiek, K. Hu, F. P. Cappuccio, and K. Yaffe, "Association between circadian rhythms and neurodegenerative diseases," *Lancet Neurol.*, vol. 18, no. 3, pp. 307–318, Mar. 2019.
- [28] M. Gombert, J. Carrasco-Luna, G. Pin-Arboledas, and P. Codoñer-Franch, "The connection of circadian rhythm to inflammatory bowel disease," *Transl. Res.*, vol. 206, pp. 107–118, Apr. 2019.
- [29] S. Kaur, A. N. Teoh, N. H. M. Shukri, S. R. Shafie, N. A. Bustami, M. Takahashi, P. J. Lim, and S. Shibata, "Circadian rhythm and its association with birth and infant outcomes: Research protocol of a prospective cohort study," *BMC Pregnancy Childbirth*, vol. 20, no. 1, pp. 1–11, Dec. 2020.
- [30] N. Goel, M. Basner, H. Rao, and D. F. Dinges, "Circadian rhythms, sleep deprivation, and human performance," *Prog. Mol. Biol. Transl. Sci.*, vol. 119, pp. 155–190, Jan. 2013.
- [31] C. E. Kline, J. L. Durstine, J. M. Davis, T. A. Moore, T. M. Devlin, M. R. Zielinski, and S. D. Youngstedt, "Circadian variation in swim performance," *J. Appl. Physiol.*, vol. 102, no. 2, pp. 641–649, Feb. 2007.
- [32] B. Edwards, H. Waterhouse, T. Reilly, and G. Atkinson, "A comparison of the suitabilities of rectal, gut, and insulated axilla temperatures for measurement of the circadian rhythm of core temperature in field studies," *Chronobiol. Int.*, vol. 19, no. 3, pp. 579–597, Jan. 2002.
- [33] S. Yoshida, H. Miyaguchi, and T. Nakamura, "Concept proof of low-energy consumption and compact ingestible thermometer based on gastric acid power generation," *IEEJ Trans. Sensors Micromach.*, vol. 138, no. 4, pp. 164–169, 2018.
- [34] S. Yoshida, H. Miyaguchi, and T. Nakamura, "Development of tablet-shaped ingestible core-body thermometer powered by gastric acid battery," *IEEE Sensors J.*, vol. 18, no. 23, pp. 9755–9762, Dec. 2018.

- [35] S. Yoshida, H. Miyaguchi, and T. Nakamura, "Proof of concept for tablet-shaped ingestible core-body thermometer with gastric acid battery," in *Proc. IEEE 1st Global Conf. Life Sci. Technol. (LifeTech)*, Mar. 2019, pp. 182–184.
- [36] H. Hafezi, T. L. Robertson, G. D. Moon, K.-Y. Au-Yeung, M. J. Zdeblick, and G. M. Savage, "An ingestible sensor for measuring medication adherence," *IEEE Trans. Biomed. Eng.*, vol. 62, no. 1, pp. 99–109, Jan. 2015.
- [37] G. P. Flores, B. Peace, T. C. Carnes, S. L. Baumgartner, D. E. Buffkin, N. R. Euliano, and L. N. Smith, "Performance, reliability, usability, and safety of the id-cap system for ingestion event monitoring in healthy volunteers: A pilot study," *Innov. Clin. Neurosci.*, vol. 13, nos. 9–10, pp. 12–19, 2016.
- [38] S. Yoshida, H. Miyaguchi, and T. Nakamura, "Prototyping of an all-pMOS-based cross-coupled voltage multiplier in single-well CMOS technology for energy harvesting utilizing a gastric acid battery," *Electronics*, vol. 8, no. 7, p. 804, Jul. 2019.
- [39] P. Nadeau, D. El-Damak, D. Glettig, Y. L. Kong, S. Mo, C. Cleveland, L. Booth, N. Roxhed, R. Langer, A. P. Chandrakasan, and G. Traverso, "Prolonged energy harvesting for ingestible devices," *Nature Biomed. Eng.*, vol. 1, no. 3, pp. 1–8, Mar. 2017.
- [40] P. M. Izdebski, H. Rajagopalan, and Y. Rahmat-Samii, "Conformal ingestible capsule antenna: A novel chandelier meandered design," *IEEE Trans. Antennas Propag.*, vol. 57, no. 4, pp. 900–909, Apr. 2009.
- [41] S. H. Lee, J. Lee, Y. J. Yoon, S. Park, C. Cheon, K. Kim, and S. Nam, "A wideband spiral antenna for ingestible capsule endoscope systems: Experimental results in a human phantom and a pig," *IEEE Trans. Biomed. Eng.*, vol. 58, no. 6, pp. 1734–1741, Jun. 2011.
- [42] R. Das and H. Yoo, "A wideband circularly polarized conformal endoscopic antenna system for high-speed data transfer," *IEEE Trans. Antennas Propag.*, vol. 65, no. 6, pp. 2816–2826, Jun. 2017.
- [43] A. Basir, M. Zada, Y. Cho, and H. Yoo, "A dual-circular-polarized endoscopic antenna with wideband characteristics and wireless biotelemetric link characterization," *IEEE Trans. Antennas Propag.*, vol. 68, no. 10, pp. 6953–6963, Oct. 2020.
- [44] S. Hayat, S. A. A. Shah, and H. Yoo, "Miniaturized dual-band circularly polarized implantable antenna for capsule endoscopic system," *IEEE Trans. Antennas Propag.*, vol. 69, no. 4, pp. 1885–1895, Apr. 2021.
- [45] Z. Chen and Z. Shen, "Planar helical antenna of circular polarization," *IEEE Trans. Antennas Propag.*, vol. 63, no. 10, pp. 4315–4323, Oct. 2015.
- [46] J. Ziegler and A. Zadehghol, "Design and simulation of a four-arm hemispherical helix antenna realized through a stacked printed circuit board structure," in *Proc. IEEE Electr. Des. Adv. Packag. Syst. Symp. (EDAPS)*, Dec. 2017, pp. 83–85.



**SHINYA YOSHIDA** (Member, IEEE) received the B.E., M.E., and Dr.E. degrees from Tohoku University, Sendai, Japan, in 2003, 2005, and 2008, respectively, all in mechanical engineering. He was a Research Associate with the World Premier International Research Center–Advanced Institute for Materials Research, Tohoku University, from 2008 to 2009, and an Assistant Professor therein, from 2009 to 2015. He has been a Project Associate Professor with the Department of Robotics, Tohoku University, since 2015. His current research interests include the development of ingestible biosensors as a health care device, and piezo-microelectromechanical systems based on piezoelectric monocrystalline thin films on Si.



**HIROSHI MIYAGUCHI** received the master's degree in electrical engineering from the Graduate School of Engineering, Keio University, in March 1979. In 1979, he joined Toshiba Corporation, where he worked on developing video devices and related LSIs. In 1987, he joined Texas Instruments Japan Ltd., and developed video signal processing DSPs and related applications. He has been associated with the Micro System Integration Center, Tohoku University, since 2011, where he focuses on the development of tactile sensor systems, massive parallel electron beam lithography, and ingestible sensor systems.



**TSUTOMU NAKAMURA** (Member, IEEE) received the master's degree from the Graduate School, Hokkaido University, in 1981. He worked on developing solid state imaging technology with Olympus Corporation. He became a specially appointed Professor at the Head Office of Enterprise Partnerships, Tohoku University, in 2015. He works on the research and development of medical devices.

...